IRAQI Academic Scientific Journals
العراقية المجلات الأكاديمية العلمية
University of Kut Journal
ISSN (E): 2616 - 7808 II ISSN (P): 2414 - 7419
js.uokut.edu.iq
k.u.c.j.sci@alkutcollege.edu.iq
Vol. 11 , Issue 1 , June 2026

Study of the Structural and Electronic Properties of Pure Polymer Polypyrrole (PPy) and Doping with TiO_2 and ZnO

Huda M. Jawad [1]

Abstract

Polypyrrole (PPy) is among the most widely used materials in many different sectors due to its electrical, optical, and mechanical properties. This work presents a study of pyrrole polymer structural and electronic properties pre- and post-doping with ZnO and TiO_2, which were investigated by performing computational calculations based on density functional theory (DFT). Interpreting theoretical vibrational spectra and finding important information about chemical bonds, functional groups, molecular structures, natural bond orbitals (NBOs), the HOMO-LUMO energy gap, density of states (DOS), and Nuclear magnetic resonance (NMR). The results exhibit functional groups present for the three structures: N-H, O-H, and C-H. The frequency of N-H increased after adding ZnO, and the frequency was greater when adding TiO_2, while the C-H stretching frequency showed a gradual increase consistent with the structures studied. The theoretically calculated energy gap was (3.865 eV) for PPy and (3.2734 eV) for PPy/ZnO, while (3.3235 eV) belongs to PPy/TiO2. Furthermore, the natural bond orbital analysis revealed that PPy/TiO2 had the highest energy among the three compounds (45.14) kcal/mol, indicating a stronger interaction between the donor and acceptor orbitals. The study found that the addition of TiO_2 and ZnO to (PPy) contributed to significant improvements in electrical conductivity, thermal stability, and electrochemical performance. This helps to improve applications in various fields, such as sensors and supercapacitors.

Keywords: Density of States, HOMO-LUMO, Polymer pyrrole

Affiliation of Author
[1] Department of Physics, College of Science, Mustansiriyah University, Iraq, Baghdad, 10001

[1]drhuda222@uomustansiriyah.edu.iq

[1] **Corresponding Author**

Paper Info.
Published: Jun. 2026

دراسة الخواص التركيبية والالكترونية لبوليمر بولي بيرول (PPy) النقي ووالمشوب ب TiO_2 و ZnO

هدى محمد جواد [1]

المستخلص

بولي بيرول (PPY) هو المادة الأكثر استخدامًا على نطاق واسع في العديد من القطاعات المختلفة يتميز بخصائصه الكهربائية والبصرية والميكانيكية. يقدم هذا العمل دراسة للخصائص التركيبية والإلكترونية لبوليمر البيرول قبل وبعد التشويب بأكسيد الزنك وثاني أكسيد التيتانيوم، وتمت هذه الدراسة من خلال إجراء حسابات نظريةبالاعتماد على نظرية الكثافة الوظيفية (DFT). وتم تفسير الأطياف الاهتزازية النظرية وإيجاد معلومات مهمة حول الروابط الكيميائية والمجموعات الوظيفية والهياكل الجزيئية ومدارات الرابطة الطبيعية (NBOs) وفجوة الطاقة HOMO-LUMO وكثافة الحالات (DOS) والرنين المغناطيسي النووي (NMR). تظهر النتائج وجود مجموعات وظيفية للهياكل الثلاثة: N-H و O-H و C-H، زاد تردد N-H بعد إضافة ZnO، وكان التردد أكبر عند إضافة TiO2، في حين كان التردد المتعلق بترددات تمدد C-H زيادة تدريجية مطابقة للهيكل الموجود. وقد تم حساب فجوة الطاقة نظرياً (3.865 إلكترون فولت) لـ PPy و (3.2734 إلكترون فولت) لـ PPy/ZnO، بينما (3.3235 إلكترون فولت) تنتمي إلى PPy/TiO2. وعلاوة على ذلك، كشف تحليل مدارات الرابطة الطبيعية أن PPy/TiO_2 كان له أعلى طاقة بين المركبات الثلاثة (45.14) كيلو كالوري/مول، مما يدل على تفاعل أقوى بين مدارات المانح والمستقبل. ووجدت الدراسة أن إضافة TiO2 و ZnO إلى (PPy) ساهمت في تحسينات كبيرة في التوصيل الكهربائي والاستقرار الحراري والأداء الكهروكيميائي. وهذا يساعد على تحسين التطبيقات في مجالات مختلفة، مثل أجهزة الاستشعار والمكثفات الفائقة.

الكلمات المفتاحية: كثافة الحالات، HOMO-LUMO، البولي بيرول

انتساب الباحث
[1] قسم الفيزياء، كلية العلوم، الجامعة المستنصرية، العراق، بغداد، 10001

[1]drhuda222@uomustansiriyah.edu.iq

[1] **المؤلف المراسل**

معلومات البحث
تأريخ النشر : حزيران 2026

Introduction

Low cost, high electrical conductivity, and thermal stability are advantages of polypyrrole (PPy), and it is also considered a valuable electrode material. [1] Polypyrrole (PPy) is an organic polymer exhibiting electrical and optical properties similar to metals and inorganic semiconductors. [2-5] Recently, (PPy) has been used in many different applications, such as electronic devices, polymeric batteries, sensors, photovoltaic devices, light-emitting diodes (LEDs), and water pollution treatment. [6-8] (Luhakhra, and Tiwari 2022) The addition of TiO_2 to PPy exhibits higher glass transition and melting temperatures than pure PPy polymer, which confirms the thermal stability. [9] (Reddy et al., 2022) The addition of TiO_2 nanoparticles also leads to changes in the surface morphology of PPy and was confirmed by scanning electron microscopy (SEM). [10] (Zenasni et al., 2024) ZnO-doped PPy also exhibits high specific capacitance and energy density, making it suitable for supercapacitor applications. [11] (Wang et al. 2022) PPy/TiO_2 composites exhibit enhanced photocurrent responses, making them effective for ultraviolet photodetectors. [12] (Anand Patil 2022) The integration of zinc/titanium dioxide with polypyrrole (PPy) aims to enhance gas sensing capabilities by leveraging the unique characteristics of these materials. [13] Polypyrrole is a heterocyclic polymer with the chemical formula H(C4H2NH)n. [14-15] It can be easily synthesized through electrochemical polymerization or oxidative polymerization. Doped (PPy) has better mechanical properties, which leads to its numerous applications in the field of biomedicine. [16-17] Figure (1-a) represents the geometric structure of (PPy). It has an electronic system that makes it important in many fields and through it, electron donors and electron acceptors are discovered. Charge transfer (CT) interactions occur between electron donors and acceptors which involve resonance with the transfer of charges between the donor and acceptor molecule. [18-19] Preparation of organic and inorganic hybrid materials based on polymers and using various transitional or non-transition metal oxides to obtain attractive mechanical and physical properties. [20-21] The electrical and optical properties of PPy can be changed by introducing electron-accepting groups into its chemical structure. As well as introducing functional groups into several sites on the pyrrole ring. These modifications affect the structural composition, including the transition energy, the width of the energy gap, and the spectrum of absorbed radiation. [22-23] Figures (1-a, 1-b, and 1-c) show the geometric structure of (PPy) doped with zinc oxide and titanium dioxide, respectively.

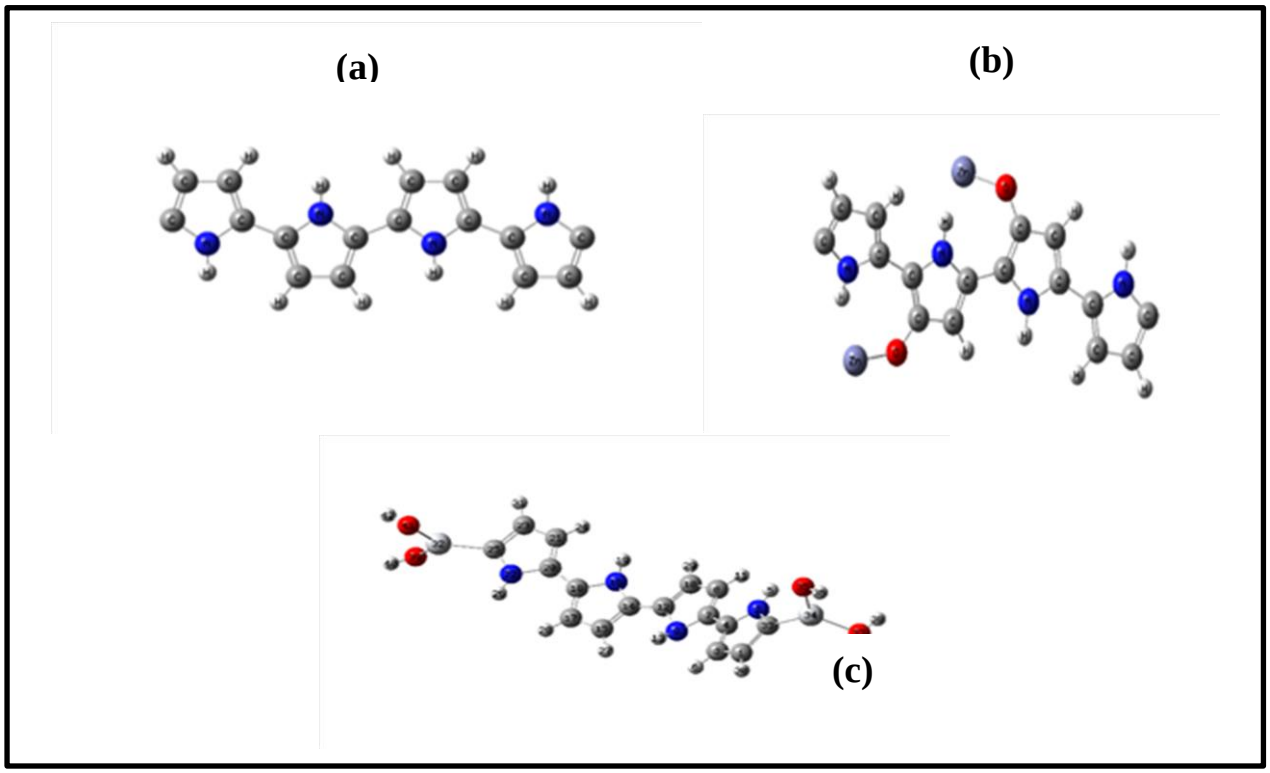

Figure (1): (a) polypyrrole (PPy), (b) PPy/ ZnO and (c) PPy/ TiO_2 using Gaussian view 06

2-Theory

Electronic structure calculations based on widely accepted quantum mechanics are used in the framework of density functional theory (DFT) to study material structures and molecular properties, as well as to study these properties at the atomic level. [24-25] Geometric optimization of polypyrrole before and after doping with titanium dioxide and zinc oxide was carried out using Gauss View 6.0 to draw the structure of the molecules. Gaussian (09) program based on (DFT) and B3LYP with 6-31G (d, p) basis set was utilized to implement the optimization process. The DFT method allows for the accurate computation of mechanical properties to clarify the characteristics of molecules and interactions and to perform calculations before and after doping. Nuclear magnetic resonance (NMR) was also studied, and in addition, ultraviolet and IR spectra analyses were taken into account. The electronic properties were studied, including the molecular orbitals, i.e., To understand stability and molecule interactions, one must know (HOMO), which is the orbital in which electrons are most present, while (LUMO) orbital in which electrons are least present. Valuable intramolecular information, such as electron delocalization and charge transfer, was obtained through natural bond orbital (NBO) analysis, as was the density of state (DOS). To calculate the electronic absorption spectra, we relied on the time-dependent DFT (TD-DFT) method. In addition, the entropy and heat capacity of the three structures were calculated. The nmrdb.org software was used to plot and analyze the NMR spectrum.

3. Results and discussion

3.1. Geometric optimization

The geometric optimization of the three compounds under study is of great importance for knowing the stability of the three structures, the course of chemical reactions, and calculating

spectra, molecular properties, and electronic properties. [26-27] Table (1) shows that the length of the bonds undergoes a slight change in the three structures due to the presence of functional groups C-H, N-H, and O-H and that the longest bond was between C-Ti and is due to the oxidation of titanium and chemical reactions and is equal to (2.3639), while the smallest bond was between N-H and equal to (1.0033).

Table (1): Bond length analyses of three structures using Gaussian (09)

	Compounds	PPy	PPy/ ZnO	PPy/TiO_2
	Bond labels	Bond length (Å)	Bond length (Å)	Bond length (Å)
1	C=C	1.4904	1.4758	1.4934
2	C-N	1.3444	1.3585	1.3452
3	C-C	1.3574	1.3705	1.3557
4	C-H	1.0737	1.0835	1.0742
5	C-N	1.4628	1.406	1.4634
6	N-H	1.0033	1.0115	1.0042
7	C=C	1.4778	1.4349	1.481
8	C-H	1.0723	1.0846	1.073
9	C-C	1.3529	1.3867	1.3498
10	C=C	1.4832	1.4234	1.481
11	C-N	1.4197	1.3954	1.4377
12	C-C	1.3543	1.4031	1.3535
13	C-H	1.0758	1.0803	1.076
14	C-N	1.4262	1.366	1.4392
15	N-H	1.001	1.0089	1.0115
16	C=C	1.4781	1.4438	1.4768
17	C-H	1.0759	1.0759	1.0769
18	C-C	1.3598	1.4116	1.3579
19	C=C	1.4781	1.4022	1.4765
20	C-N	1.4262	1.3806	1.4352
21	C-C	1.3543	1.4087	1.3557
22	C-H	1.0759	1.0808	1.0765
23	C-N	1.4197	1.3768	1.4273
24	N-H	1.001	1.0166	1.0105
25	C=C	1.4832	1.4789	1.4771
26	C-H	1.0758	1.0752	1.0745
27	C-C	1.3529	1.3744	1.36
28	C=C	1.4778	1.4409	1.4469

29	C-N	1.4628	1.4144	1.4726
30	C-C	1.3574	1.3657	1.3839
31	C-H	1.0723	1.0841	1.0681
32	C-N	1.3444	1.3477	1.3153
33	N-H	1.0033	1.0133	1.0119
34	C=C	1.4904	1.4841	1.5497
35	C-H	1.0737	1.0836	
36	Zn- O		1.9796	
37	Zn-O		1.9669	
38	C-O		1.3683	
39	C-O		1.3874	
40	TiO			1.8991
41	TiO			1.9468
42	C-Ti			2.3639
	O-H			1.054
	O-H			0.9821

3.2 Vibrational assignments

Interpreting theoretical vibrational spectra and finding important information about chemical bonds, functional groups, and molecular structures. [28-29] The functional groups present for the three structures were: N-H, O-H, and C-H, which are mentioned with their frequencies in Table (2). The functional groups determined from the calculations in the structures PPy, PPy/ZnO and PPy/TiO_2, respectively, and the frequency of N-H increased after adding ZnO, and the frequency was greater when adding TiO_2, while the C-H stretching frequency showed a gradual increase consistent with the structures studied.

Table (2): The table shows the theoretical analysis of vibrations using Gaussian (09).

functional groups	Frequency (cm^{-1})		
	PPy	PPy/ ZnO	PPy / TiO_2
N-H	3200	3534.017	3434.308
O-H			3609.067
C-H	2800.98	3251.012	2877.56

3.3 Ultraviolet (UV) analysis

To understand the electronic characteristics and know the absorption behavior of the three structures in the ultraviolet region, the ultraviolet spectrum was analyzed. [30-31] The calculations included energy, wavelength, oscillator strength, and percentage contribution through excitation-type analysis. Table (3) shows the transition of electrons from the ground state to the excited state from $S_0 \rightarrow S_1$, and $S_0 \rightarrow S_2$, and the outputs showed that the highest wavelength was for (PPy / TiO_2) then (PPy /ZnO) and finally it was (PPy).

From Table (3), the excitation energy gradually decreases for the three structures, where the energy is highest in (PPy) and decreases in the two compounds PPy/ZnO and PPy/TiO_2, respectively, due to the interactions between PPy, ZnO, and TiO_2, which leads to an increase in interference between the electronic states of the two compounds. As this table indicates, the wavelength is shorter in PPy while it gradually increases in ZnO and TiO_2, it was also noted that the structure has a higher oscillator strength in PPy than PPy/ZnO and PPy/Tio_2. The optimization was $S_0 \rightarrow S_1$ and $S_0 \rightarrow S_2$, showing the transition of electrons from the ground state to a higher excited state.

Table (3): UV analysis computed theoretically using Gaussian (09).

structures	Excitation Type	Energy (eV)	Wavelength (nm)	Percentage contribution (%)	Oscillator Strength	Transition (f)
PPy	$S_0 \rightarrow S_1$	0.6935	1787.77	55→56(90.19)	0.7604	H → L
	$S_0 \rightarrow S_2$	0. 8009	1776.28	54→56(73.29)	0.4501	H - 1 → L
PPy / ZnO	$S_0 \rightarrow S_1$	0.4510	1488.02	55→56(90.19)	0.3320	H → L
	$S_0 \rightarrow S_2$	0.5332	2250.18	54→56(38.25)	0.3169	H - 1 → L
PPy / TiO_2	$S_0 \rightarrow S_1$	0.3946	3141.77	55→56(84.31)	0.2006	H → L
	$S_0 \rightarrow S_2$	0.4697	2639.87	54→56(54.88)	0.0769	H - 1 → L

3.3 Molecular orbitals

The sensitivity, conductivity and electronic properties were estimated by analyzing the molecular orbitals of the structures under study. To know the sensing capabilities of these structures, Table (4) shows (HOMO) and (LUMO) energy, and that the gap energy is equal to the energy difference between HOMO and LUMO. When the energy gap is small, it indicates an increase in the value of conductivity and sensitivity, high chemical reactivity and low stability due to electronic transfers. These values were close to the experimental values in the literature. This may be because the boundary conditions are neglected in theoretical calculations, and some studies have shown that the difference between experimental and calculated values. The theoretically calculated band gaps were (3.865 eV) for PPy and (3.2734 eV) for PPy/ZnO, while (3.3235 eV) belongs to PPy/TiO_2. There is a great convergence between experimental and theoretical values. [32-35] Figure (2) represents the HOMO-LUMO and energy gap for three structures. The energy gap, HOMO, and LUMO, which are regarded as quantum descriptors in a variety of chemical and biochemical systems, are used in many applications.

Table (4): **Energy gap analyses calculations using Gaussian (09)**

System	HOMO (a.u)	LUMO (a.u.)	Energy Gap (eV)
PPy	-0.17988	-0.03784	3.8
PPy/ZnO	-0.4312	-0.3109	3.2
PPy/TiO2	-0.17998	-0.03784	3.3

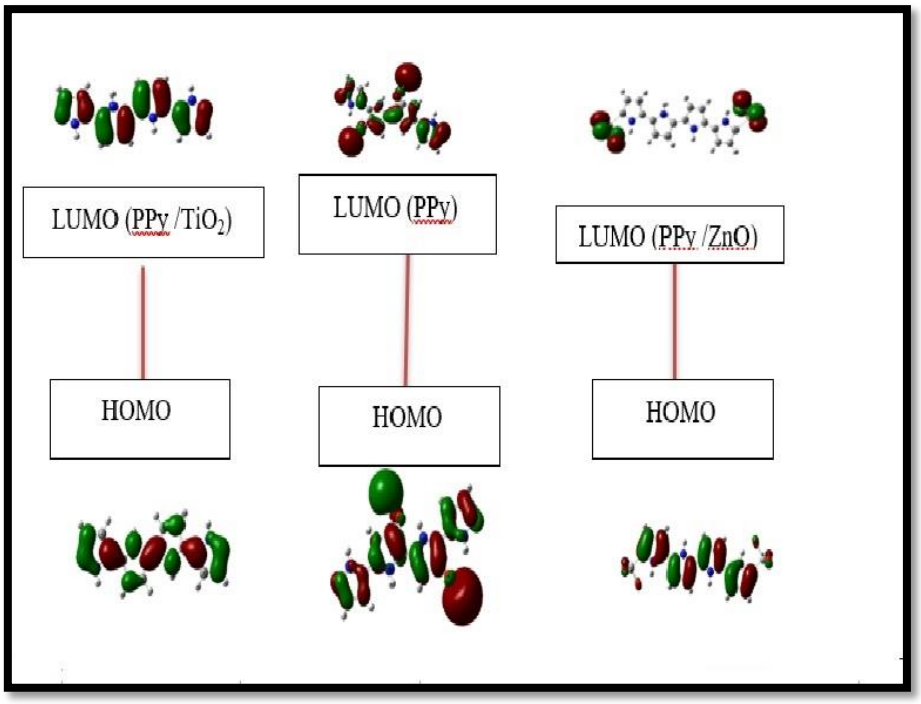

Figure (2): Representation of the HOMO-LUMO of three structures using Gaussian view 06.

To obtain more parameters that provide additional understanding of intermolecular interactions, stability, and optical and electrical properties of the structures, the Koopmans approximation was utilized. Numerous indicators have been used, like electronegativity (χ), which displays the ability of an atom or set of atoms to draw an electron. Chemical hardness (η) expresses the resistance of an atom or group of atoms to transferring charge. As for (EA), it represents the measure of affinity and acceptance of an electron to obtain additional electrons from the systems around them. Chemical softness (σ) is the probability of an atom accepting one or more electrons. The chemical system's unexcited ionization potential (IP) was also studied. [36- 38] These parameters explain the electrical and optical properties in addition to intermolecular interactions and stability. Table (5), we note that these studied formulations showed a pattern of sensitivity decreasing as follows: PPy/ZnO > PPy > PPy /TiO_2.

Table (5): HOMO – LUMO, analyses calculations using Gaussian (09).

Compound	IP	EA	χ	η	-μ	σ
PPy	0.17988	0.03784	0.10886	0.07102	-0.10886	7.13266
PPy/ZnO	0.4312	0.3109	0.37105	0.06015	-0.37105	8.31255
PPy/TiO_2	0.17998	0.03784	010891	0.08098	-010891	7.0353

3.4 Natural bond orbital

Natural bond orbital (NBO) analysis is a way to understand the nature of the orbital connection between donor and acceptor in nanocomposites. The molecular orbitals resulting from interactions in molecules when a charge is transferred from the full donor to the empty acceptor are explained based on the natural bond orbital decomposition (NBO). [39] Second-order perturbation theory is important in estimating natural bond orbital (NBO) energies. This technique helps in understanding chemical bonding by simplifying the complex Schrödinger equation. In table (6) one can see donor (I) and acceptor (J) with transition second order energy E2 and energy gap (Ei – Ej) and F is the standard deviation. The tabulated results for all compounds showed π → π* interactions, where the stability energies for PPy were 17.29 kcal/mol, 21.25 kcal/mol, 15.12 kcal/mol, 45.43 kcal/mol, and 16.93 kcal/mol. The interaction energy associated with the resonance of the electron donor molecule to the electron acceptor for π C_1- N_3 →π* C_5- C_8, π C_2 – C_4 →π* C_1 - N_3, πC_{18}- C_{20} →π* C_{13}- C_{17}, πC_{21}- C_{24} →π* N_{26}- C_{29} respectively. As for PPy/ZnO, the interaction energies associated with resonance for charge transfer were recorded at 28.61 kcal/mol, 20.85 kcal/mol, 13.87 kcal/mol, 21.35 kcal/mol, and 20.85 kcal/mol. The electron donor molecule to the electron acceptor for π C_1 - C_2 →π* C_2 - C_4, π C_2- C_5 →π* C_5 - C_8, π N_{24}- C_{27} →π* C_{20} – C_{22}, π C_{23} – C_{22} →π* indicating that these values are affected by the presence of two ZnO. As for PPy/TiO_2, the energies associated with the resonance of electron transitions were 45.14 kcal/mol, 28.43 kcal/mol, 27.04 kcal/mol, and 10.66 kcal/mol. For the next transitions π C_3- C_4→π*, C_3- C_1, π C_8 – C_7 →π* C_7 – N_9, π C_{14} – C_{15} →π* C_{14} -N_{16}, andπ O_{36} →π* Ti_{38}, indicating that these values are affected by the presence of two TiO_2.

Table (6): Second-order perturbation theory analysis of the Fock matrix in NBO basis in PPy, PPy/ZnO and PPy/TiO_2 using Gaussian (09)

Compound	Donor (i)	type	Acceptor (j)	type	E (2) kcal/mol	E(j)-E(i) (a.u.)	F(j,i) a.u.
PPy	C_1- N_3	π	C_5- C_8	π*	17.29	0.34	0.073
	C_2 – C_4	π	C_1 - N_3	π*	21.25	0.30	0.072
	C_{18}- C_{20}	π	C_{13}- C_{17}	π*	15.12	0.30	0.064
	C_{21}- C_{24}	π*	C_{25}- C_{27}	π	21.85	0.02	0.060
	C_{21}- C_{24}	π*	N_{26}- C_{29}	π*	16.93	0.02	0.034
PPy/ZnO	C_1 - C_2	π	C_2 - C_4	π*	28.61	0.22	0.078
	C_2- C_5	π	C_5 - C_8	π*	20.85	0.28	0.072
	C_8- C_9	π	C_5 - C_8	π*	13.87	0.32	0.062
	N_{24}- C_{27}	π	C_{20} – C_{22}	π*	21.35	0.35	0.082
	C_{21}- C_{24}	π	C_{25}- C_{27}	π*	42.43	0.30	0.071
PPy/Tio_2	C_{21}- C_{24}	π	C_{25}- C_{27}	π*	45.14	0.13	0.087

	$C_8 – C_7$	π	$C_7 – N_9$	π*	28.43	0.22	0.082
	$C_{14} – C_{15}$	π	C_{14} -N_{16}	π*	27.04	0.22	0.081
	O_{36}	π	Ti_{38}	π*	10.66	0.49	0.067

3.5 Density of States (DOS)

The density of states (DOS) is of great significance in comprehending the electronic characteristics of materials and knowing the available states of the electron inside the atom for certain energy levels. It can describe DOS as the number of electron states per unit volume per unit energy, which depends on energy. Atoms participating in the compound, such as carbon (C), hydrogen (H), and Nitrogen (N) were carefully examined, in addition to its related elements such as (O), (Zn), and (Ti). Fig. (3) exhibits the DOS of the three compounds. The properties, stability and electronic effect of these compounds come from many factors, including hydrogen bond interactions, which have an effective role in the behavior and stability of the compounds. Its use is attributed to many fields, including drug design, catalysis, and materials science. [40-41]

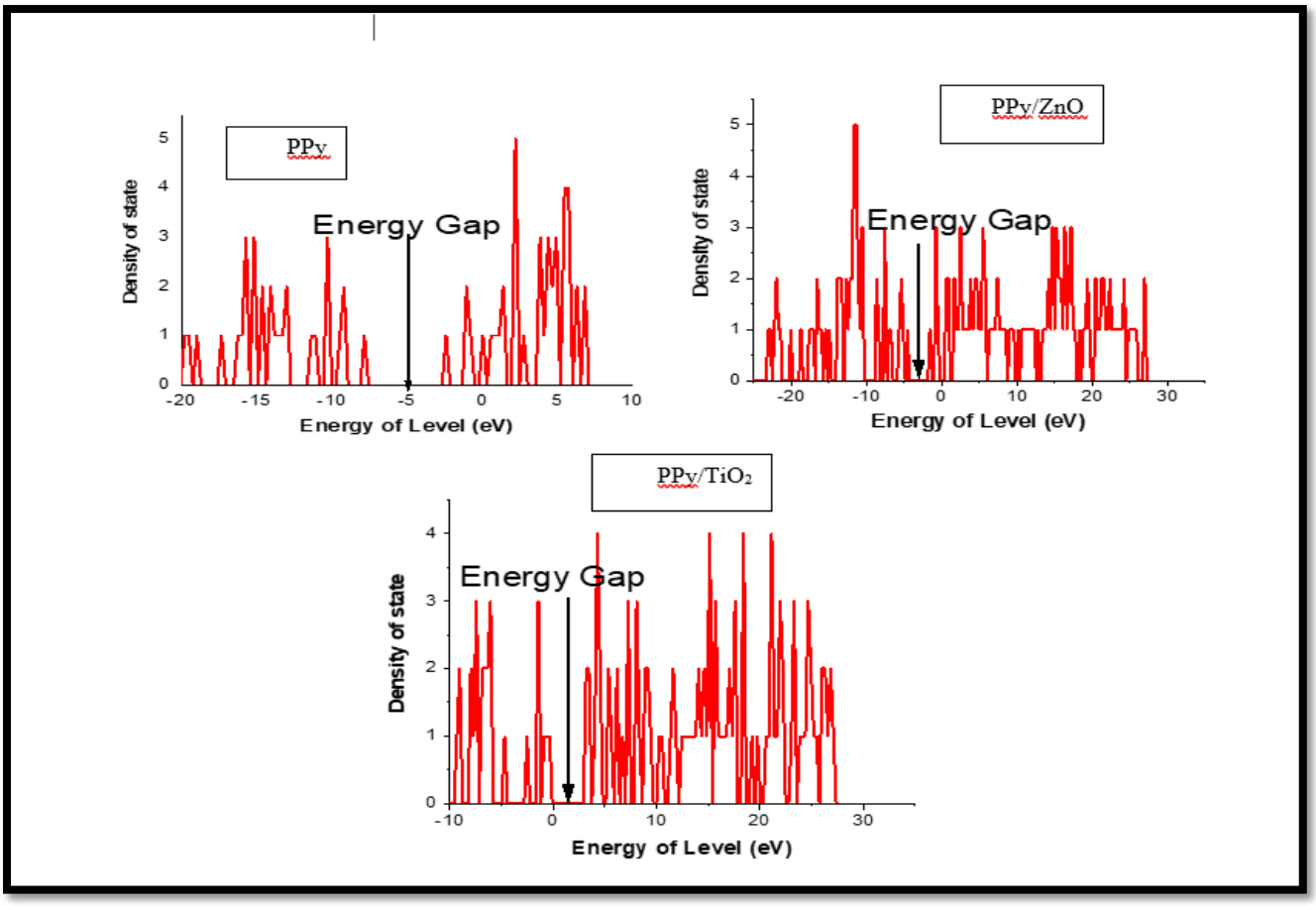

Figure (3): Indicates (DOS) for the three compounds using Gaussian view 06

3.6 Nuclear magnetic resonance (NMR)

Nuclear magnetic resonance (NMR) spectroscopy is the most widely used method to study molecular structure and determine the molecule's interaction with energy and the production of different energy states. In addition to determining the functional groups have different energy values for resonance absorption, the number of protons representing each signal, and the number of protons connected to adjacent carbons, i.e. Spin-Spin splitting. Fig. (4-a, 4-b, and 4-c) represent (NMR) of three compounds. The energy axis is called a **δ** (delta) axis and the units are given in parts per million (ppm) [42]. The nmrdb.org software was used to plot and analyses the NMR spectrum [38]. Fig. (4-a) Signals were found at (1.5 - 2) ppm for pure PPy, and these signals belong to the atoms. (N_{26}, C_{29}, H_{28}, H_{23}, H_{12}, H_{16}, C_{27}, H_{31}, and H_{15}. The second set of peaks was found at (3) ppm, corresponding to C_{29}, C_{30}, C_1, C_2, H_{16}, H_7. The peaks that appear at (3.5) include the following atoms C_5, C_8, C_{17}, C_{13}, C_{24}, C_{21}, C_5, and N3. As for Fig. (4-b), which represents PPy/ZnO, ^{13}C NMR: **δ**- 56.6-56.6 (4C, 56.6 (s), 56.6 (s), 56.6 (s), 56.6 (s)), 71.7-71.8 (6C, 71.7 (s), 71.7 (s), 71.7 (s), 71.7 (s), 71.7 (s), 71.7 (s)), 73.9-74.0 (2C, 73.9 (s), 73.9 (s)), 123.8-123.8 (2C, 123.8 (s), 123.8 (s)), 133.6-133.8 (2C, 133.7 (s), 133.7 (s)). Where **δ** , where (s) denotes a singlet. Fig. (4-c) shows NMR: **δ** 71.7 (2C, s), 110.0-110.1 (6C, 110.1 (s), 110.1 (s), 110.1 (s)), 123.8 (2C, s), 133.6-133.8 (6C, 133.7 (s), 133.7 (s)).

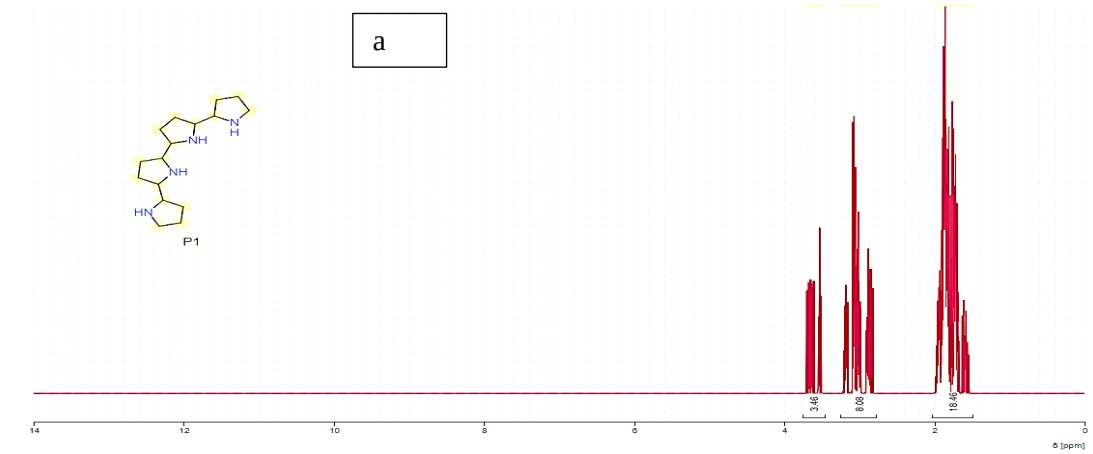

***δ*(ppm)**

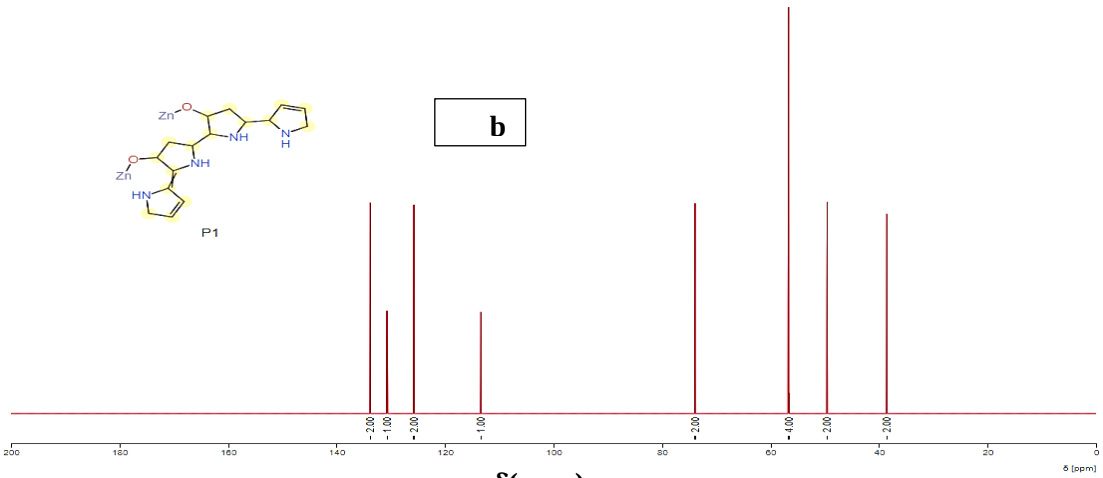

***δ*(ppm)**

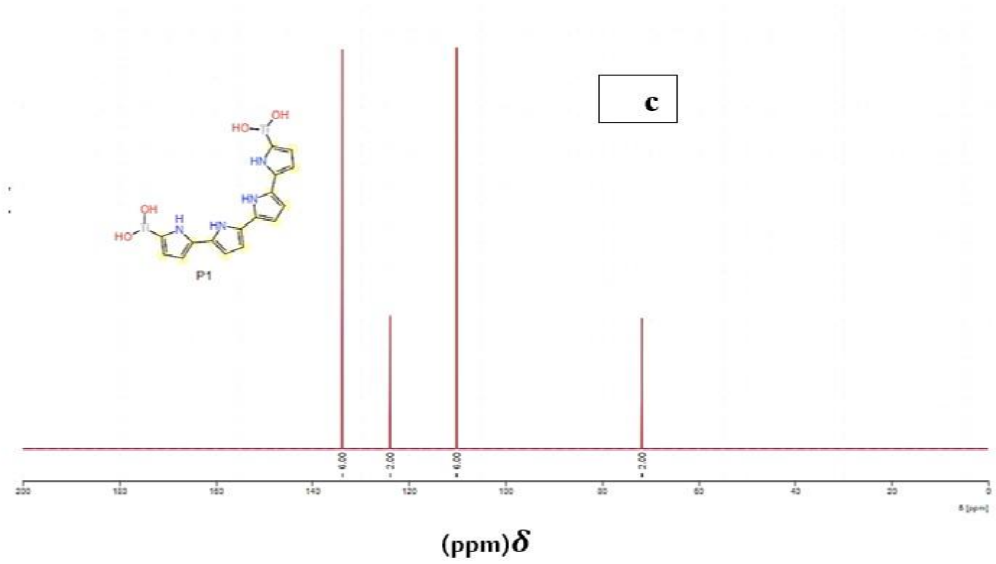

Figure (4): (NMR) of three compounds [43]

4. Conclusions

Finally, the study of the spectral properties and UV-vis analysis provided valuable insights into the interactions of TiO_2/ZnO with (PPy) using DFT and Gaussian (09) to optimize the geometry of the structural details that affect the electronic and optical properties of the composite material. The analysis results showed that the interaction between TiO_2/ZnO with (PPy) enhances stability and improves electronic properties, making them useful for applications in photovoltaic cells, sensors, or photocatalysis. The study indicates the importance of molecular interactions of composite materials, which play an important role in their functional properties and suitability for various technological applications.

Acknowledgement The authors thank Mustansiriyah University (www.uomustansiriyah.edu.iq) in Baghdad, Iraq, for its support in the present work. This research did not receive any grant from the University.

Competing interests

The authors declare that they have no competing interests.

References

[1].Iqbal MJ, Iqbal MZ, Fazal A. Graphene/Polymer Composite Application on Supercapacitors. In Innovations in Graphene-Based Polymer Composites. Woodhead Publishing .2022; pp. 583-610. https://doi.org/10.1016/B978-0-12-823789-2.00022-4.

[2]. Upadhyay LSB, Rana S, Kumar N. Nanomaterials in tissue engineering: Applications and challenges. Advances in Nanotechnology-Based Drug Delivery Systems. 2022; 533-554. https://doi.org/10.1016/B978-0-323-88450-1.00018-1

[3]. Mohamed F, Rehim MA, Hameed TA, Turky G. Optical Properties and Dielectric Relaxation of Polypyrrole and Poly (3-Hexylthiophene). Physica Scripta.2023;

98(12): 125912. DOI 10.1088/1402-4896/ad049c.

[4]. Elumalai P, Charles J. Investigation of Structural and Optical Properties of Ternary Polyaniline–Polypyrrole–Nickel Oxide (PANI-PPy-NiO) Nanocomposite for Optoelectronic Devices. Polymer International. 2023; 72(2): pp176-188. https://doi.org/10.1002/pi.6456.

[5]. Milu MMH, Anjum A, Rahman MA, Hoque ME. Influence of Compatibilizer on Free Vibration and Damping Behavior of Polymer Biocomposites. In Vibration and Damping Behavior of Biocomposites.2022; pp. 137-155. https://doi.org/10.1201/9781003173625.

[6]. Pang AL. Arsad A, Ardani MR, Ismail N E, Julkapli N M, Ahmadipour M. Exploring the impact of Oxidant Rratio on Polypyrrole Properties: Electrical, Optical, and Adsorption Behaviour. Inorganic Chemistry Communications. 2023; 155. https://doi.org/10.1016/j.inoche.2023.111052.

[7]. Amin KF, Sen A, Hoque ME. Polymer Nanocomposites for Energy. In Advanced Polymer Nanocomposites.2022; pp. 335-372. https://doi.org/10.1016/B978-0-12-824492-0.00007-6.

[8]. Hoque ME, Shafoyat MU. Self-Healing Polymer Nanocomposite Films and Coatings. In Polymer Nanocomposite Films and Coatings. 2024; pp. 181-217. https://doi.org/10.1016/B978-0-443-19139-8.00010-3.

[9]. Luhakhra Neha, TIWARI, Sanjiv Kumar. Thermal and Electrical Study of Polypyrrole and TiO2/Polypyrrole Composite. In: International Conference on Nanotechnology: Opportunities and Challenges. Singapore: Springer Nature Singapore, 2022; pp. 299-305.

[10]. Reddy Ruhma, et al. Advancements in TiO2-based photocatalysis for environmental remediation: strategies for enhancing visible-light-driven activity. Chemosphere, 2023; 140703. https://doi.org/10.1016/j.chemosphere.2023.140703.

[11]. Zhao Feng, et al. Polypyrrole doped zirconium dioxide composite as electrode material for supercapacitor applications. Indian Journal of Physics, 2024; pp 1-8.

[12]. Wang Huan, et al. Polypyrrole Film Deposited-TiO2 Nanorod Arrays for High Performance Ultraviolet Photodetectors. Chemosensors, 2022; 10.7: 277.

[13]. Anand Patil and Nirdosh Patil. Fabrication, Characterization and NH3 Sensing Properties of Zinc Supported TiO2 Doped Polypyrrole Nanocomposite Thin Films, Asian Journal of Chemistry, 2022; 34(12), pp.3263-3268

[14]. Yu EH, Sundmacher K. Enzyme Electrodes for Glucose Oxidation Prepared by Electropolymerization of Pyrrole. Process Safety and Environmental Protection. 2007;85(5): pp 489-493. https://doi.org/10.1205/psep07031.

[15]. Mao J, Zhang, Z. Polypyrrole as Electrically Conductive Biomaterials: Synthesis, biofunctionalization, potential applications and challenges. Cutting-Edge Enabling Technologies for Regenerative Medicine.2018; pp 347-370. https://doi.org/10.1007/9.

[16]. Huang ZB, Yin GF, Liao XM. Gu JW. Conducting Polypyrrole in Tissue Engineering Applications. Frontiers of Materials Science.

2014; 8: pp39-45. https://doi.org/10.1007/s11706-014-0238-8.

[17]. Borges MH, Nagay BE, Costa RC, Souza JGS, Mathew MT, Barão VA. Recent Advances of Polypyrrole Conducting Polymer Film for Biomedical Applications: Toward a viable Platform for Cell-Microbial Interactions. Advances in colloid and interface science. 2023; 314: ttps://doi.org/10.1016/j.cis.2023.102860.

[18]. Lakkad, A, Baindla N. Tigulla P. Synthesis, Spectroscopic and Computational Studies of Charge-Transfer Complexation Between 4-Aminoaniline and 2, 3-Dichloro-5, 6-Dicyano-1, 4-Benzoquinone. Journal of Solution Chemistry. 2017; 46:pp 2171-2190. https://doi.org/10.1007/s10953-017-0685-9.

[19]. Varukolu M, Palnati M, Nampally V, Gangadhari S, Vadluri M, Tigulla P. New Charge Transfer Complex Between 4-Dimethylaminopyridine and DDQ: Synthesis, Spectroscopic Characterization, DNA binding analysis, and density functional theory (DFT)/time-dependent DFT/natural transition Orbital Studies. ACS Omega. 2021;7(1): pp 810-822. https://doi.org/10.1021/acsomega.1c05464.

[20]. Batool A, Kanwal, F, Imran, M, Jamil T, Siddiqi S A. Synthesis of Polypyrrole/Zinc Oxide Composites and Study of their Structural, Thermal and Electrical Properties. Synthetic Metals. 2012; 161(23-24): pp2753-2758. https://doi.org/10.1016/j.synthmet.2011.10.016 .

[21]. Folorunso O, Hamam Y, Sadiku R, Ray SS, Adekoya GJ. Synthesis Methods of Borophene, Graphene-Loaded Polypyrrole Nanocomposites and their Benefits for Energy Storage Applications: A brief overview. FlatChem.2021; 26: https://doi.org/10.1016/j.flatc.2020.100211.

[22]. Mizera A, Grabowski S J, Ławniczak P, Wysocka-Żołopa M, Dubis AT, Łapiński AA. Study of the Optical, Electrical and Structural Properties of Poly (Pyrrole-3, 4-Dicarboxylic Acid). Polymer. 2019; 164: pp142-153. https://doi.org/10.1016/j.polymer.2018.12.056.

[23]. Ha NN, Cuong NT, Van Hung H, Hung HM, Trung VQ. Electronic Properties of the Polypyrrole-Dopant Anions ClO 4− and MoO 4 2−: a Density Functional Theory Study. Journal of Molecular Modeling. 2017; 23 (336): pp 1-8. https://doi.org/10.1007/s00894-017-3509-3.

[24]. Burke K. Perspective on Density Functional Theory. The Journal of Chemical Physics. 2012; 136: https://doi.org/10.1063/1.4704546.

[25]. Jones RO. Density Functional Theory: Its Origins, Rise to Prominence, and Future. Reviews of Modern Physics.2015; 87(3): https://doi.org/10.1103/RevModPhys.87.897.

[26]. Maurer RJ, Freysoldt C, Reilly AM, Brandenburg JG, Hofmann OT, Björkman T, Lebègue S, Tkatchenko A. Advances in Density-Functional Calculations for Materials Modeling. Annual Review of Materials Research. 2019; 49: pp1-30. https://doi.org/10.1146/annurev-matsci-070218-010143.

[27]. Kumara K, Kumar AD, Naveen S, Kumar KA, Lokanath NK. Synthesis, Spectral Characterization, and X-ray Crystal Structure Studies of 3-(Benzo [d][1, 3] Dioxol-5-yl)-5-(3-Methylthiophen-2-yl)-4, 5-Dihydro-1H-Pyrazole-1-Carboxamide: Hirshfeld Surface, DFT and Thermal Analysis. Journal of

Molecular Structure. 2018; 1161: pp 285-298. https://doi.org/10.1016/j.molstruc.2018.02.068 .

[28]. Zierkiewicz W, Privalov T. A Theoretical Study of the Essential Role of DMSO as a Solvent/Ligand in the Pd (OAc) 2/DMSO Catalyst System for Aerobic Oxidation. Organometallics. 2005; 24(24): pp 6019-6028. https://doi.org/10.1021/om0506217.

[29]. Adindu EA, Godfrey OC, Agwupuye EI, Ekpong BO, Agurokpon DC, Ogbodo SE, Louis H. Structural Analysis, Reactivity Descriptors (HOMO-LUMO, ELF, NBO), Effect of Polar (DMSO, EtOH, H2O) Solvation, and Libido-Enhancing Potential of Resveratrol by Molecular Docking. Chemical Physics Impact. 2023; 7: https://doi.org/10.1016/j.chphi.2023.100296.

[30]. Hossain A. Spectral Simulation and Method Design of Camouflage Textiles for Concealment of Hyperspectral Imaging in UV-Vis-IR Against Multidimensional Combat Background. The Journal of the Textile Institute. 2023; 114(2): pp 331-342. https://doi.org/10.1080/00405000.2022.2027074.

[31]. Makhlouf J, Louis H, Benjamin I, Ukwenya E, Valkonen A, Smirani, W. Single Crystal Investigations, Spectral Analysis, DFT Studies, Antioxidants, and Molecular Docking Investigations of Novel Hexaisothiocyanato Chromate Complex. Journal of Molecular Structure.2023; 1272: https://doi.org/10.1016/j.molstruc.2022.134223.

[32]. Chowdhury MSH, Khan, MMR, Shohag MRH, Rahman, S., Paul, S. K., Rahman, M. M., ... & Rahman, M. M., Easy synthesis of PPy/TiO2/ZnO composites with superior photocatalytic performance, efficient supercapacitors and Nitrite Sensor. Heliyon. 2023; 9(9): https://doi.org/10.1016/j.heliyon.2023.e19564.

[33]. Kandulna R, Choudhary RB. Robust Electron Transport Properties of PANI/PPY/ZnO Polymeric Nanocomposites for OLED Applications. Optik. 2017;144: pp 40-48. https://doi.org/10.1016/j.ijleo.2017.06.094.

[34]. Jawad HM, Jasim FA. Theoretical Investigations on the Natural Bond Orbital, HOMO-LUMO, Contour Maps, and Energy Gap of Diatrizoate. In AIP Conference Proceedings.2024; 3097(1): https://doi.org/10.1063/5.0209811.

[35]. Jawad HM, Kadhim AM, Jasim FA. Study of Molecular Structure, vibrational spectroscopy, and HOMO-LUMO of Bromocyclohexane, Iodobenzene, and Chlorobenzene by Density Functional Theory. In AIP Conference Proceedings.2024; 3097(1): https://doi.org/10.1063/5.0209812.

[36]. Ouafy HE, Aamor M, Oubenali M, Mbarki M, Haimouti AE. Ouafy TE. Molecular Structure, Electrostatic Potential and HOMO, LUMO Studies of 4-Aminoaniline, 4-Nitroaniline and 4-Isopropylaniline by DFT. Science & Technology Asia. 2022; 27(1): pp 9-19. https://tci-thaijo.org/index.php/SciTechAsia.

[37]. Frau J, Flores-Holguín N, Glossman-Mitnik D. Chemical Reactivity Theory and Empirical Bioactivity Scores as Computational Peptidology Alternative Tools for the Study of Two Anticancer Peptides of Marine Origin. Molecules. 2019; 24(6): https://doi.org/10.3390/molecules24061115.

[38]. Rebaz O M E R, KOPARIR P, QADER IN, AHMED L. Structure Reactivity Analysis for Phenylalanine and Tyrosine. Cumhuriyet Science Journal. 2021; 42(3): pp 576-585. http://dx.doi.org/10.17776/csj.881654.

[39]. Gangadharan, R, Sampath Krishnan, S. Natural Bond Orbital (NBO) Population Analysis of 1-Azanapthalene-8-ol. Acta Physica Polonica A.2014; 125(1): PP18-22. 10.12693/APhysPolA.125.18.

[40]. Yoshino M, Morinaga M, Shimode A, Okabayashi K, Nakamatsu H, Sekine R. A Universal Relation Between Electron Density Minima and Ionic Radii in Ceramics. Materials transactions1968; 45(7): pp1968-1972. https://doi.org/10.2320/matertrans.45.1968.

[41]. Jain A, Ong S P, Hautier G. Commentary: The Materials Project: A Materials Genome Approach to Accelerating Materials. APL Materials.2013; 1 (1): https://doi.org/10.1063/1.4812323.

[42]. Kesküla A, Heinmaa I, Tamm T, Aydemir N, Travas-Sejdic J, Peikolainen A L, Kiefer R. Improving the Electrochemical Performance and Stability of Polypyrrole by Polymerizing Ionic Liquids. Polymers. 2020; 12(1): https://doi.org/10.3390/polym12010136.

[43]. http://nmrdb.org/13c/index.shtml?v=v2.138.0#